

Crystallisation of amorphous spray-dried precursors in the Al_2O_3 – SiO_2 system

André Douy*

CNRS, Centre de Recherches sur les Matériaux à Haute Température, 1D, Avenue de la Recherche Scientifique, 45071 Orléans, Cedex 02, France

Received 1 December 2004; received in revised form 18 February 2005; accepted 25 February 2005

Available online 10 May 2005

Abstract

The crystallisation of amorphous precursors has been studied in the whole range of composition in the Al_2O_3 – SiO_2 system. The amorphous precursors have been obtained by hydrolysing TEOS directly in a diluted aqueous solution of aluminium nitrate, spray drying the clear solution and heating the resulting powder. Up to 70 mol % Al_2O_3 , only mullite crystallises around 980–1000 °C; between 70 and 80 mol % Al_2O_3 mullite and spinel crystallise together; and for more than 80 mol % Al_2O_3 only spinel is formed. In the 70–80 mol % Al_2O_3 range of composition, when both mullite and spinel crystallise, low heating favours the crystallisation of mullite and it is nearly possible to crystallise only mullite from a 75 mol % Al_2O_3 sample. By rapid heating it is also possible to crystallise only spinel from the same 75 mol % Al_2O_3 precursor. The enthalpy and the activation energy for crystallisation are maximum for 60–80 mol % Al_2O_3 . Heating the samples up to 1700 °C for 1 h, the phase equilibrium is not reached, particularly when both mullite and spinel crystallise together, and θ - Al_2O_3 is still present.

© 2005 Elsevier Ltd. All rights reserved.

Keywords: Powders chemical preparation; Crystallisation; Mullite

1. Introduction

Mullite is the only thermodynamically stable phase in the Al_2O_3 – SiO_2 system at ambient pressure. Its excellent high-temperature properties such as good mechanical strength, low thermal expansion coefficient and high creep resistance make it an attractive ceramic material for high-temperature mechanical applications. Because of its low dielectric constant mullite is also a good candidate as electronic packaging substrate in substitution for alumina.^{1,2}

Its formation, from amorphous precursors, glasses and also kaolin, has been extensively studied. For amorphous precursors having the bulk composition close to $3\text{Al}_2\text{O}_3 \cdot 2\text{SiO}_2$, the crystallisation path depends on the scale of homogeneity in the amorphous phase. For the more homogeneous specimens, when the aluminium and silicon polyhedra are the most intimately mixed, crystallisation occurs at about 980 °C with

a sharp exothermic peak on DTA experiments, and mullite is the only crystallised phase. When the chemical homogeneity in the precursor decreases, mullite and a spinel phase that is a solid solution of defect transition alumina can crystallise together at the same temperature (~980 °C) and by ~1250 °C this spinel has transformed to mullite. Going on increasing the scale of heterogeneity only the spinel phase may crystallise at 980 °C and transforms into mullite through a second exotherm around 1250 °C. And for the more heterogeneous specimens, no exotherm is observed at 980 °C, but a broad exotherm at about 1300 °C may traduce the formation of mullite from a transitional alumina phase and a siliceous phase.

Mullite exists as a solid solution with the general formula $\text{Al}_{4+2x}\text{Si}_{2-2x}\text{O}_{10-x}$ where x represents the number of oxygen vacancies per unit cell ranging from ca 0.17 to 0.59.³ The compositional variation is based on the exchange of $\text{O}^{2-} + 2\text{Si}^{4+} \rightarrow 2\text{Al}^{3+} + \square$ which introduces one oxygen vacancy. Mullite derives from sillimanite Al_2SiO_5 ($x=0$) by replacing silicon atoms by aluminium atoms in tetrahedral environment. Mullite formed at 980 °C is always richer in

* Tel.: +33 2 38 25 55 26; fax: +33 2 38 63 81 03.

E-mail address: douy@cnrs-orleans.fr.

alumina than the bulk precursor. It has been called “tetragonal mullite” but in fact has an orthorhombic structure with the cell parameters a and b being very close. By increasing temperature a progressive contraction of the a -parameter indicating a decrease of the alumina content, is generally observed, and a composition very close to $3\text{Al}_2\text{O}_3 \cdot 2\text{SiO}_2$ is reached after firing to about 1400°C . This implies that the low temperature mullite coexists with an amorphous silica-rich phase. The phase separation has been shown to occur before crystallisation by Huling and Messing.⁴ They reported that all quenched aluminosilicate glasses are phase separated and that phase separation proceeds more rapidly than crystallisation for amorphous mullite composition gels and glasses. For glasses, phase separation has been explained by immiscibility in the liquid state, and even several mullites of different compositions have been evidenced in the same sample after crystallisation of a glass.⁵

Considerable work has been devoted to the crystallisation of mullite from amorphous precursors processed by various syntheses or from kaolin or glasses. Among these syntheses, spray pyrolysis at 350 – 650°C of aluminium nitrate and TEOS in a water–methanol solution led to crystallisation of mullite at $\sim 980^\circ\text{C}$.⁶ The nebulisation at 150°C of an aerosol of hydrolysed Al-*sec*-butoxide and TMOS solution led to the formation of both spinel and mullite.⁷ Spinel was the first crystalline phase from high temperature ($\geq 900^\circ\text{C}$) decomposition of an aerosol of Al nitrate and fumed silica⁸ or from ultrasonic spray pyrolysis at 900°C of aqueous solutions of Al nitrate and silicic acid.⁹ In the present work we have studied the crystallisation of amorphous spray-dried powders in the whole range of compositions in the Al_2O_3 – SiO_2 system. Spray-drying aqueous solutions being a less usual and less known process for mullite synthesis,^{10,11} the kinetics of crystallisation have been determined for comparison with usual processes. Mullite being the only stable binary oxide in this system, we have been interested by the structural evolution of the crystallised phases with temperature up to reaching the phase equilibria.

2. Experimental procedure

2.1. Samples preparation

The amorphous precursors were prepared by a spray-drying and calcination process. For this, tetraethoxysilane (TEOS), $\text{Si}(\text{OC}_2\text{H}_5)_4$ (Fluka, $\geq 99\%$) was hydrolysed into a carefully titrated aqueous solution of aluminium nitrate ($\sim 1\text{M}$). The resulting clear solution was spray-dried using a laboratory apparatus (Büchi 190 mini spray-drier equipped with a 0.5mm nozzle). The drying air was heated to 200 – 210°C . A part of the powder was used for the thermogravimetric study of its decomposition and the rest was heated in a ventilated furnace at $5^\circ\text{C}/\text{min}$ to 800°C for 5 h in order to completely decompose the nitrate ions, resulting in an amorphous powder. Each preparation was made for around

5 g of final oxide from 200 – 250mL of solution. For structural characterisation samples were heated under air atmosphere in an electric furnace at $10^\circ\text{C}/\text{min}$ to a determined temperature (1000 – 1700°C) and annealed for 1 h at this temperature before cooling at $20^\circ\text{C}/\text{min}$.

2.2. Characterisation

The thermogravimetric analyses (TGA) of the spray-dried powders were carried out on a TAG 24 Setaram apparatus at $5^\circ\text{C}/\text{min}$ in air atmosphere.

The DSC experiments (Setaram MultiHTC apparatus) were performed at different heating rates under air atmosphere on powders annealed at 800°C . 100 – 200mg of sample were used for each experiment, in alumina crucibles. The DSC temperature calibration was carried out for different heating rates melting high purity metals. The enthalpy accuracy measurement was within $\pm 10\%$. The activation energy of crystallisation was calculated from the exothermic peak using the Kissinger equation:¹²

$$\ln\left(\frac{\alpha}{T_p^2}\right) = -\frac{E_a}{RT_p} + C,$$

where α is the heating rate (K/min), E_a is the activation energy for crystallisation (J/mol), R is the gas constant, T_p is the exothermic peak temperature (K) and C is a constant. T_p was determined at the top of the peak and a same weight of powder was used for each experiment for a given composition. The heating rates were 0.4 , 1 , 2.5 , 6 and $12^\circ\text{C}/\text{min}$.

The XRD powder patterns were collected at room temperature on a Philips PW1729 diffractometer ($\text{Cu K}\alpha$ radiation) in a flat plate geometry. Data were recorded in the 2θ range 10 – 70° by steps of 0.02° with a scan time of 1 or 10 s per step.

3. Results and discussion

3.1. Synthesis

The process of synthesis is very simple and has proved to be efficient in the preparation of chemically homogeneous powders crystallising directly into mullite for the $3\text{Al}_2\text{O}_3 \cdot 2\text{SiO}_2$ composition^{10,11} as it was also the case for spray pyrolysis of aluminium nitrate and TEOS in water–methanol solution.⁶ TEOS is not miscible with aqueous solutions, but mixed under stirring with a diluted solution of aluminium nitrate, the acidity of the latter solution ($\text{pH} \sim 2$) catalyses its hydrolysis into soluble silicic acid. The transformation of the starting mixture into a perfectly clear solution is a direct visualisation of its hydrolysis. This is achieved within half an hour. At acidic pH, low concentration and room temperature, the polycondensation of silicic acid into silica gel is very low.¹³ This molecular solution is then abruptly transformed into a powder by spray drying, in-

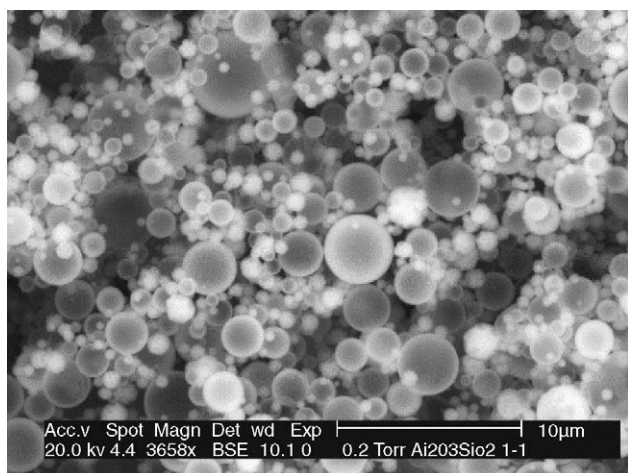


Fig. 1. Scanning electron micrograph of a spray-dried powder (50 mol % Al_2O_3).

ensuring a good dispersion of Al and Si elements inside the resulting solid.

The spray-dried powder is then heated in order to completely decompose the nitrate ions and create Si–O–Al bonds.¹⁴ The morphology of spray-dried powders is typical of such a process.¹⁵ The powders are made of hollow spheres, with sizes ranging around 0.5–5 μm as determined by scanning electron microscopy (Fig. 1).

In Fig. 2a and b are reported the thermal analysis curves of the spray-dried powders with 50 and 90 mol % Al_2O_3 contents as typical examples. Under the same experimental conditions, aluminium nitrate alone is partially decomposed into an oxynitrate after spray drying.¹⁶ On the TG trace the major part of the weight loss of the spray-dried sample corresponds to the decomposition of this oxynitrate in two steps (140 and 260 $^\circ\text{C}$ on the derivative curve DTG for the 90 mol % Al_2O_3 , Fig. 2b). The weight loss is practically ended at about 400 $^\circ\text{C}$. The total weight loss depends upon the composition. It increases with the Al_2O_3 content (Fig. 2a and b) since the aluminium oxynitrate has to be decomposed while for the silica part only water molecules have to be released from the condensation of silanol groups. There is a supplementary weight loss around 980 $^\circ\text{C}$, at the same temperature that a sharp exothermic peak corresponding to the crystallisation is observed on the DSC trace. This weight loss is due to the release of the last residues, hydroxyl groups and products of decomposition of nitrate ions entrapped inside the spheres. The specific surface areas of these spray-dried powders is usually low¹⁰ suggesting that the spheres are rather tight and these residues can escape only during the structural reorganisation occurring at crystallisation or under the preceding viscous flow conditions. This behaviour around crystallisation varies strongly with the composition of the samples. The specific weight loss going with the crystallisation is not perceptible for the silica-rich samples. It is well marked on the derivative curve (DTG) for the 50 mol % Al_2O_3 sample (Fig. 2a). It has been measured to 0.93% of the mass of the sample annealed

at 800 $^\circ\text{C}$. The importance of the weight loss at high temperature increases with the alumina content, being higher than 5% for 75–95 mol % Al_2O_3 , with a maximum of 7.4% for 85 mol % Al_2O_3 , relative to the weight of samples calcined at 800 $^\circ\text{C}$. It occurs at a temperature closely related to that of the crystallisation studied by DSC at the same heating rate, at the exception of the pure alumina sample. For the latter one there is no specific weight loss accompanying the crystallisation but there is also a rather important release of matter at a higher temperature. It is obvious that the weight loss going on with the crystallisation is related to the presence of intimately dispersed silica in the aluminous amorphous matrix.

3.2. Crystallisation

Whatever the composition, only one exothermic peak corresponding to the crystallisation was observed on the DSC analyses. Takei et al.,¹⁷ studying the crystallisation of ultra-quenched glasses of different compositions, noted a splitting of the exothermic peak for 25, 30 and 36 mol % Al_2O_3 compositions. For their 25 mol % Al_2O_3 sample, two exothermic peaks were separated by 15 $^\circ\text{C}$ (986 and 1001 $^\circ\text{C}$) at a heating rate of 5 $^\circ\text{C}/\text{min}$. They assigned these two peaks to crystallisations from two separated phases, due to spinodal decomposition of the liquid. Okada and Otsuka¹⁸ reported similar splitting for Al_2O_3 – SiO_2 gels with similar range

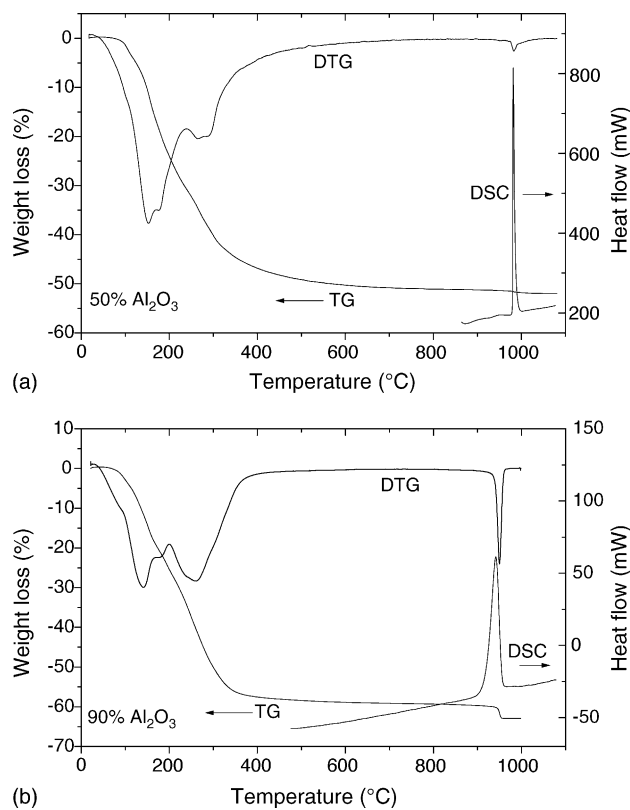


Fig. 2. (a) DSC and TG analyses of the 50 mol % Al_2O_3 spray-dried powder; heating rate: 5 $^\circ\text{C}/\text{min}$. (b) DSC and TG analyses of the 90 mol % Al_2O_3 spray-dried powder; heating rate 5 $^\circ\text{C}/\text{min}$.

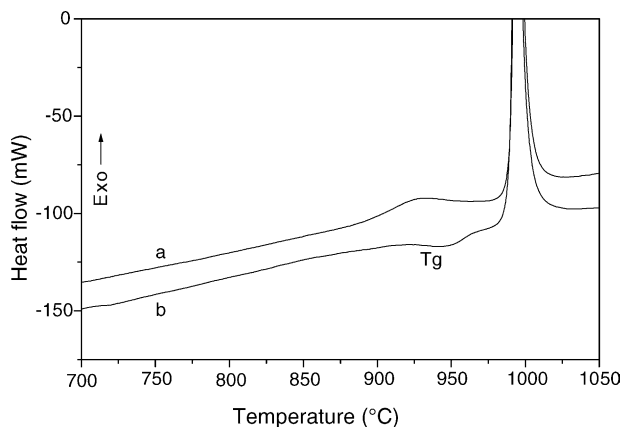


Fig. 3. DSC analyses of the 25 mol % Al_2O_3 powder: (a) normal DSC of the sample annealed at 800 °C; (b) DSC of the sample quenched after being heated to 950 °C.

of compositions. We did not observe a similar behaviour for spray-dried samples in the same range of compositions. Only a weak exothermic bump could be observed on the DSC traces before the crystallisation peak for the silica-rich compositions. In Fig. 3 are reported the DSC analyses of the spray-dried sample with 25 mol % Al_2O_3 . For the sample just annealed at 800 °C (a) there is a little bump at 900–950 °C before the sharp peak of crystallisation. The XRD diagram of the specimen quenched after heating to 950 °C revealed no crystallised phase. If this sample, quenched just after being heated to 950 °C, is heated again (b) the bump is replaced by a weak thermal effect that resembles more to the glass transition phenomenon for glasses. Moreover this thermal effect is reproducible for samples quenched just after, as far as crystallisation has not occurred. Since no particular weight loss is observed by TG analysis, the exothermic bump at the first heating step is attributed to a structural reorganisation in the sample, a relaxation of the network. At the second heating ramp, the weak thermal effect traduces the glass transition (T_g) of the sample and is followed by the strong exothermic peak of crystallisation. This thermal effect has been observed in our laboratory for many spray-dried aluminosilicate compositions, sometimes associated with a slight weight loss. The gel to glass transition has also been reported in the literature.^{19–21}

3.2.1. Crystallisation of mullite or spinel

The variation of the temperature of crystallisation with the composition, determined at a heating rate of 5 °C/min, is reported in Fig. 4. After just heating to 1000 °C, with increasing the alumina content in the sample, only mullite can be detected as crystallised phase up to compositions approaching 70 mol % Al_2O_3 . For the silica-rich samples a bump around 20–25° on the XRD diagrams traduces the presence of an amorphous phase, which should be amorphous silica. For compositions with 80 mol % or higher Al_2O_3 content only the broad lines of the traditional spinel phase are present on the patterns. For the intermediate compositions mullite

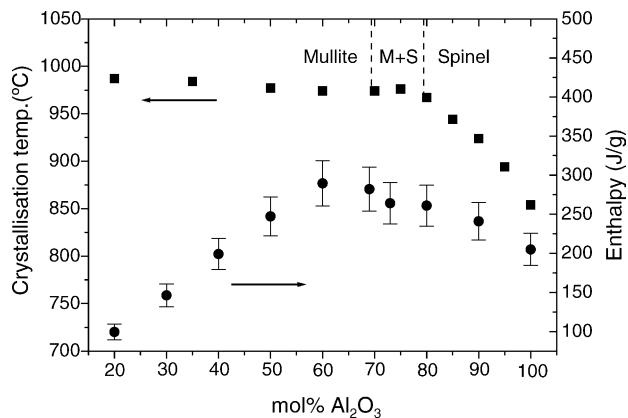


Fig. 4. Temperatures of crystallisation at 5 °C/min, domains of composition where mullite, mullite and spinel, or spinel crystallise, and enthalpy of crystallisation.

and spinel both crystallise. The presence of both mullite and spinel for samples in the 70–80 mol % Al_2O_3 range of composition traduces the chemical heterogeneity of the precursor at the nanoscopic scale. For ideally homogeneous precursors the limit composition leading to the crystallisation of only mullite for silica-richer samples or only spinel for alumina-richer samples may be estimated around 75 mol % Al_2O_3 . When mullite and spinel crystallise together, the heating rate may favour the formation of mullite or spinel, as they have different kinetics of crystallisation. This is illustrated on Fig. 5 for the same precursor having a content of 75 mol % Al_2O_3 crystallised by (a) putting directly at 1100 °C, (b) heating at 5 °C/min and (c) slow heating at 1 °C/min up to 950 °C for 10 h. By very rapid heating (a) only a trace of mullite is detected on the XRD diagram, showing that, unless an appreciable part of silica is present in the amorphous state, practically 25 mol % SiO_2 can be inserted in the $\gamma\text{-Al}_2\text{O}_3$ solid solution. On the other hand by slow heating only a little amount of spinel is crystallised (c) showing that by lowering the heating rate only mullite can be crystallised from alumina-richer samples. However a very slow heating rate is unable to

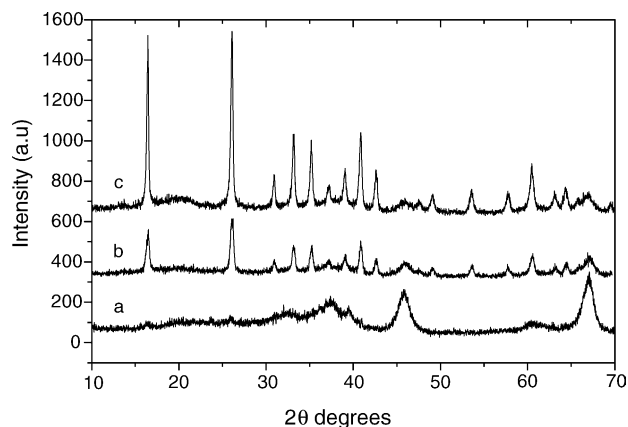


Fig. 5. XRD patterns of the 75 mol % Al_2O_3 sample after crystallisation at different heating rates: (a) putting directly at 1100 °C; (b) 5 °C/min; (c) 0.1 °C/min to 950 °C for 10 h.

crystallise mullite for higher alumina content specimens for which only spinel normally crystallises. For example, in the case of 80 mol % Al_2O_3 no trace of mullite is detected after heating at $0.1^\circ\text{C}/\text{min}$. Crystallisation into mullite or spinel is governed by the local structure in the amorphous phase and particularly the local environment of the aluminium atoms.¹⁴

3.2.2. Crystallization temperature

The crystallisation temperature (Fig. 4) slightly decreases for the silica-rich precursors when the alumina content increases, then slightly increases for the compositions corresponding to the crystallisation of both mullite and spinel and then sharply decreases when only spinel crystallises. This trend for variation of the temperature of crystallisation with the composition has been already reported.^{11,17,18,22,23} Starting from pure alumina sample that crystallises into $\gamma\text{-Al}_2\text{O}_3$, the incorporation of silicon atoms in the network leads to an increase of the crystallisation temperature of the $\gamma\text{-Al}_2\text{O}_3$ solid solution, and this temperature regularly increases with the silica content. Many cations are known to delay the crystallisation of alumina and stabilise the temperature domain of transition aluminas. It is the case for example with alkaline-earth cations Ca^{2+} , Sr^{2+} and Ba^{2+} .²⁴ The two effects, increase of the crystallisation temperature and increase of the stability domain of the $\gamma\text{-Al}_2\text{O}_3$ solid solution, increase with the ionic radius of the cation, Ba^{2+} being the most efficient. In the case of calcium up to almost 33 mol % CaO can be incorporated into the $\gamma\text{-Al}_2\text{O}_3$ solid solution.¹⁶ In the present study, more than 20 mol % SiO_2 , possibly 25 mol % SiO_2 , can be incorporated into the $\gamma\text{-Al}_2\text{O}_3$ solid solution.

3.2.3. Enthalpy of crystallisation

The enthalpies of crystallisation were determined from the DSC experiments and corrected for the weight loss observed during the experiments. The variation of the enthalpy with the global composition of the sample is represented in Fig. 4. With increasing the alumina content, the enthalpy increases regularly in the domain of crystallisation of mullite and decreases in the domain of crystallisation of spinel. The maximum values are found in the 60–70 mol % Al_2O_3 range of composition, where a maximum amount of mullite crystallises. The value -290 J/g for 60 mol % Al_2O_3 (-124 kJ/mol if the formula were $3\text{Al}_2\text{O}_3 \cdot 2\text{SiO}_2$) is close to other reported values in the literature for the crystallisation of homogeneous gels of the same composition: -112 kJ/mol ,²⁵ -105 kJ/mol .²⁶ It can be noted that there is no significant difference in enthalpy between crystallisation of mullite (60–70 mol % Al_2O_3) and crystallisation of spinel (80 mol % Al_2O_3).

3.2.4. Activation energy

The activation energies for crystallisation (Fig. 6) were determined varying the heating rate from 0.4 to $12^\circ\text{C}/\text{min}$. Several values have been reported for nucleation-growth of mullite. Most of the data are in the range 700 – 1350 kJ/mol , whether crystallisation occurs from glasses,^{5,17} polymeric

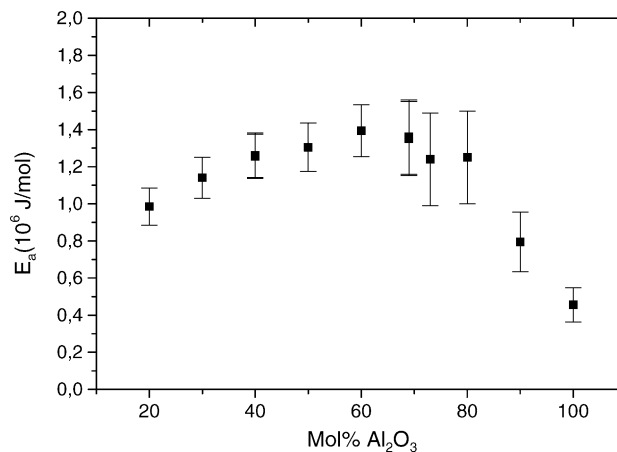


Fig. 6. Variation of the activation energy for crystallisation with the composition of the powder.

xerogels,²⁷ diphasic xerogels,²⁸ hybrid xerogels²⁹ or microcomposites particles.³⁰ Okada et al.²⁷ reported that energy for nucleation-growth of spinel from a 80 mol % Al_2O_3 xerogel (1092 kJ/mol) was similar to the energy for nucleation-growth of mullite from a 60 mol % Al_2O_3 xerogel (1202 kJ/mol). Our study agrees with their conclusion. The maximum value is found for 60 mol % Al_2O_3 (Fig. 6), 1394 kJ/mol , the activation energy for nucleation-growth remains high as long as mullite and spinel crystallize together, and even when only spinel crystallize (1250 kJ/mol for 80 mol % Al_2O_3). The activation energy decreases significantly only for higher alumina content.

The amorphous precursors were made of hollow spheres, and just before crystallisation, when the powder should normally sinter by a viscous flow, the spheres blow up to release the entrapped gases. The inflation of the powders varies with the composition, the maximum of swelling being observed in the 70–90 mol % Al_2O_3 range of composition corresponding also to the maximum of weight loss observed on TG analyses. As this inflation increases also with increasing the heating rate, at the higher heating rate of the study, $12^\circ\text{C}/\text{min}$, the powders within this composition range blow up and partially get out of the crucible. The DSC results were not valuable in this case and the energies of activation were deduced from heating rates up to $6^\circ\text{C}/\text{min}$ using smaller amounts of powder. The studied samples were amorphous precursors annealed at 800°C , but in fact no variation was found in the determination of the activation energy of crystallisation for the same precursor just heated to 450°C or annealed for 5 h at 850°C . We agree with Johnson et al.,⁵ in their study on devitrification of quenched mullite, that the specimens were fully nucleated by the time they reached 850°C .

3.3. Structural evolution with temperature

It is well known that mullite just crystallised at low temperature, near 980°C , is metastable. It is always richer in alumina, even when the amorphous precursor is a silica-rich

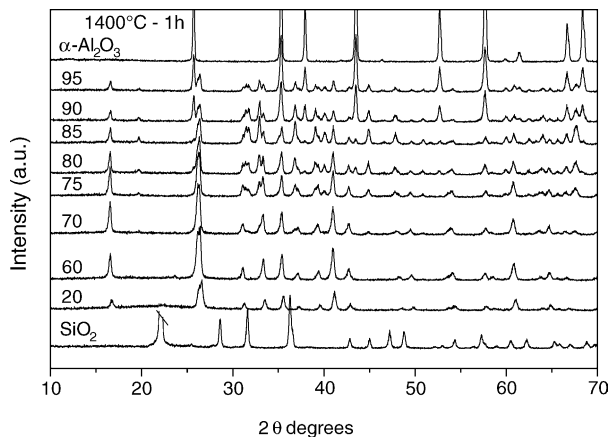


Fig. 7. XRD patterns of samples heated at 10 °C/min to 1400 °C for 1 h.

phase, its composition being usually close to $2\text{Al}_2\text{O}_3 \cdot \text{SiO}_2$. By further heating the latter gradually evolves to a composition nearest to $3\text{Al}_2\text{O}_3 \cdot 2\text{SiO}_2$ by reacting with a vitreous silica phase. On the other hand if a spinel phase is crystallized around 980 °C, this phase is also metastable, and it reacts also with a silica-rich amorphous phase to form mullite or mullite and $\alpha\text{-Al}_2\text{O}_3$ depending on the global composition. The structural evolution of the low temperature crystallised phases in the $\text{Al}_2\text{O}_3\text{-SiO}_2$ system, with increasing temperature, is very complex and is worth to be studied in detail. It is considered generally that by 1300–1400 °C the phase equilibrium is practically reached. In a first approach we have just identified the crystalline phases present after a specific thermal treatment, heating at 10 °C/min to a determined temperature, annealing for 1 h and cooling the sample to room temperature. The oven was limited to 1700 °C. Some XRD diagrams are represented on Figs. 7 and 8. It is obvious that the phase equilibria are far to be reached for these samples at 1400 °C or even higher. On Fig. 9 are reported the temperatures to be reached for each studied composition for just having on the XRD diagrams the crystalline phases expected from the phase diagram (i.e. cristobalite, mullite

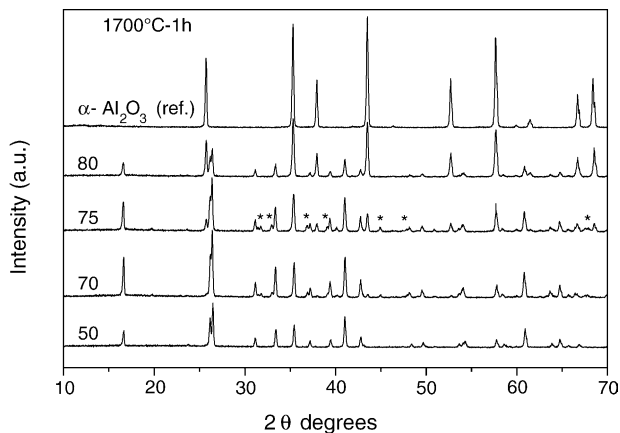


Fig. 8. XRD patterns of samples heated at 10 °C/min to 1700 °C for 1 h; *, $\theta\text{-Al}_2\text{O}_3$.

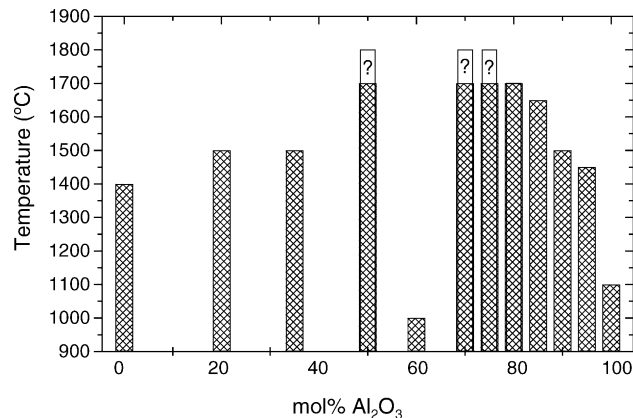


Fig. 9. Temperatures required for having on the XRD patterns of the spray-dried powders all the crystalline phases expected from the phase diagram: cristobalite, mullite and $\alpha\text{-Al}_2\text{O}_3$. For 50 mol % Al_2O_3 cristobalite is not detected after 1 h at 1700 °C, and for 70 and 75 mol % Al_2O_3 a transition alumina is still present. For 60 mol % Al_2O_3 , although mullite is the only crystalline phase at 1000 °C, phase equilibrium is far to be reached.

and $\alpha\text{-Al}_2\text{O}_3$). For 60 mol % Al_2O_3 for example this temperature is indicated at 1000 °C, although an amorphous silica phase is present and the composition of the mullite phase has to evolve on further heating. For the pure silica sample cristobalite is crystallised only at 1400 °C, but after the same treatment it is not detected on the diagram of the 20 mol % Al_2O_3 (80 mol % SiO_2) sample (Fig. 7). A very minor amount of mullite phase dispersed in a silica matrix is sufficient to delay the crystallisation of cristobalite. This phenomenon is even more significant for the 50 mol % Al_2O_3 sample (Fig. 8): after heating for 1 h at 1700 °C only mullite is detected on the XRD diagram, and no cristobalite, although the composition of this sample is out of the mullite solid solution stable domain (58.5–62.8 mol % Al_2O_3).³¹ With 50 mol % SiO_2 in the sample and considering all the aluminium atoms in mullite, a composition of 60 mol % Al_2O_3 for mullite heated to 1700 °C would imply that a third of the silicon atoms remain in amorphous silica and that the sample would be a mixture of one mole of amorphous SiO_2 for one mole of crystallised $3\text{Al}_2\text{O}_3 \cdot 2\text{SiO}_2$.

The same phenomenon can be observed for the alumina-rich samples. For the pure alumina sample, $\alpha\text{-Al}_2\text{O}_3$ is the only phase present after 1 h at 1100 °C. But with only 5 mol % SiO_2 (95 mol % Al_2O_3), transition alumina is still present after a thermal treatment of 1400 °C for 1 h (Fig. 7), and by increasing the silica content, higher temperatures are required for obtaining a mixture of mullite and $\alpha\text{-Al}_2\text{O}_3$ according to the phase diagram: 1650 °C for 85 mol % Al_2O_3 and 1700 °C for 80 mol % Al_2O_3 . For the samples with 70 and 75 mol % Al_2O_3 transition alumina, $\theta\text{-Al}_2\text{O}_3$, is still present (Fig. 8) and higher temperature or higher duration of treatment are thus necessary to transform this remaining metastable phase. These samples were crystallised by heating at 10 °C/min and higher heating rate even favour the amount of transition alumina (Fig. 5). Many metal oxides have been shown to be efficient in retarding the transformation of transition alumina,

Si, Zr, Th, Cr, alkaline earths and rare earths being among the most effective metals. But never so high temperatures have been observed for transition alumina, their temperature domain being generally limited to 1300–1400 °C. Horiuchi et al.³² studying compositions with 2.5–10 wt.% SiO₂, found that 5 wt.% SiO₂ (8.2 mol %) was the most effective content for suppressing phase transformation; the θ phase remained even after heating at 1400 °C for 1 h. The occurrence of θ -Al₂O₃, resisting to a treatment of 1700 °C for 1 h, should be specific of the type of synthesis, that is to spray-drying aqueous solutions of aluminium nitrate and silicic acid. The high content of silica in the samples giving rise to these high temperature resisting metastable phases, 25–30 mol % SiO₂ is also unusual. This temperature delay in phase transformation may be due to the small size of the crystallites of transition alumina solid solution, stabilised by silicon atoms, well dispersed in a matrix of mullite and their difficulty to grow and evolve towards stable phases. This particular behaviour may be enhanced by the small thickness of the walls of the hollow spheres. Similarly the presence of amorphous silica in samples submitted to the same thermal treatment may be due to the small size of the silica domains embedded in a mullite matrix. More information about this peculiarity should be obtained from a detailed study of these spray-dried powders by high resolution electron microscopy.

4. Conclusions

Hydrolysing TEOS into an aqueous solution of aluminium nitrate and then spray drying this solution is a very simple, rapid and reliable process for the synthesis of chemically homogeneous amorphous precursors in the Al₂O₃ – SiO₂ system. It allows to easily explore the whole range of composition. Whatever the composition, only a single crystallisation exotherm can be observed. The crystallised phases are mullite up to 70 mol % Al₂O₃, mullite and a spinel phase for compositions between 70 and 80 mol % Al₂O₃, and only the spinel phase for the alumina-richer samples. When both mullite and spinel crystallise together, rapid heating favours the crystallisation of spinel and it is possible to crystallise a γ -Al₂O₃ solid solution with practically up to 25 mol % SiO₂. By slow heating it is also possible to crystallise only mullite from a nearly 75 mol % Al₂O₃ sample. The enthalpy and the activation energy for crystallisation evolve regularly and are the higher for 60–80 mol % Al₂O₃ compositions, that is in the composition domain where a maximum amount of mullite or mullite and silica-rich spinel are crystallised. The most spectacular result is the persistence of amorphous silica and transition alumina after treatment at 1700 °C for 1 h, that is far higher than usually observed. This is probably due to the sizes of the silica domains and of the transition alumina crystallites embedded in a matrix of mullite, and the morphology of the powders made of hollow spheres.

Beyond these results this study is worth to be completed by a detailed high resolution electron microscopy analysis of

the evolution with temperature. Some aspects of the crystallisation itself have to be detailed: the important loss of residues occurring with the crystallisation of silica-rich γ -Al₂O₃ solid solution, the determination of the composition of each mullite phase just crystallised through the measure of the cell parameters, the evolution of this composition with the composition of the precursor and its evolution with temperature, the local structure of the precursors via high resolution solid state ²⁷Al and ²⁹Si MAS NMR spectroscopy, a comparison with the high temperature liquid state of the Al₂O₃–SiO₂ system and the relation between crystallisation and liquid immiscibility.

Acknowledgement

F. Bouzin is gratefully acknowledged for his assistance.

References

1. Somiya, S., Davis, R. F. and Pask, J. A., Ceramic transactions. *Mullite and Mullite Matrix Composites*, vol. 6. The American Ceramic Society, Westerville, OH, 1990.
2. Schneider, H., Okada, K. and Pask, J. A., *Mullite and Mullite Ceramics*. Wiley, New York, 1994.
3. Cameron, W. E., Mullite: a substituted alumina. *Am. Mineral*, 1977, **62**, 747–755.
4. Huling, J. C. and Messing, G. L., Chemistry-crystallization relations in molecular mullite gels. *J. Non-Cryst. Solids*, 1992, **147–148**, 213–221.
5. Johnson, B. R., Kriven, W. M. and Schneider, J., Crystal structure development during devitrification of quenched mullite. *J. Eur. Ceram. Soc.*, 2001, **21**, 2541–2562.
6. Kanzaki, S., Tabata, H., Kumazawa, T. and Ohta, S., Sintering and mechanical properties of stoichiometric mullite. *J. Am. Ceram. Soc.*, 1985, **68**, C6–C7.
7. Ocana, M., Sanz, J., Gonzales-Carreno, T. and Serna, S., Spherical mullite particles prepared by hydrolysis of aerosols. *J. Am. Ceram. Soc.*, 1993, **76**, 2081–2085.
8. Moore, K. A., Cesarano III, J., Smith, D. M. and Kodas, T. T., Synthesis of submicrometer mullite powder via high-temperature aerosol decomposition. *J. Am. Ceram. Soc.*, 1992, **75**, 213–215.
9. Janackovic, Dj., Jokanovic, V., Kostic-Gvozdenovic, Lj., Zivkovic, Lj. and Uskokovic, D., Synthesis, morphology, and formation mechanism of mullite particles produced by ultrasonic spray pyrolysis. *J. Mat. Res.*, 1996, **11**, 1706–1716.
10. Jaymes, I. and Douy, A., Homogeneous mullite-forming powders from spray-dried aqueous solutions. *J. Am. Ceram. Soc.*, 1992, **75**, 3154–3156.
11. Jaymes, I., Douy, A., Gervais, M. and Coutures, J. P., Crystallization in the SiO₂–Al₂O₃ system from amorphous powders. *J. Sol–Gel Sci. Technol.*, 1997, **8**, 415–418.
12. Kissinger, H. E., Reaction kinetics in differential thermal analysis. *Anal. Chem.*, 1957, **29**, 1702–1706.
13. Iler, R. K., *The Chemistry of Silica*. Wiley, New York, 1979.
14. Jaymes, I., Douy, A., Massiot, D. and Coutures, J. P., Characterization of mono- and di-phasic mullite precursor powders prepared by aqueous routes. *J. Mat. Sci.*, 1996, **31**, 4581–4589.
15. Messing, G., Zhang, S.-C. and Jayanthi, G., Ceramic powder synthesis by spray pyrolysis. *J. Am. Ceram. Soc.*, 1993, **76**, 2707–2726.
16. Douy, A. and Gervais, M., Crystallizations from amorphous precursors in the calcia–alumina system. A differential scanning calorimetry study. *J. Am. Ceram. Soc.*, 2000, **83**, 70–76.

17. Takei, K., Kameshima, Y., Yasumori, A. and Okada, K., Crystallization kinetics of mullite from Al_2O_3 - SiO_2 glasses under non-isothermal conditions. *J. Eur. Ceram. Soc.*, 2001, **21**, 2487–2493.
18. Okada, K. and Otsuka, N., Characterization of the spinel phase from SiO_2 - Al_2O_3 xerogels and the formation process of mullite. *J. Am. Ceram. Soc.*, 1986, **69**, 652–656.
19. Puyané, R., James, P. F. and Rawson, H., Preparation of silica and soda-silica glasses by the sol-gel process. *J. Non-Cryst. Solids*, 1980, **41**, 105–115.
20. Brinker, C. J. and Scherer, G. W., Sol \rightarrow gel \rightarrow glass: 1. gelation and structure. *J. Non-Cryst. Solids*, 1985, **70**, 301–322.
21. Zelinski, J. J., Fabes, B. D. and Uhlmann, D. R., Crystallization of sol-gel derived glasses. *J. Non-Cryst. Solids*, 1986, **82**, 307–313.
22. Wang, Y. and Thomson, W. J., Mullite formation from nonstoichiometric slow hydrolyzed single phase gels. *J. Mater. Res.*, 1995, **10**, 912–917.
23. McHale, J. M., Yürekli, K., Dabbs, D. M., Navrotsky, A., Sundaresan, S. and Aksay, A., Metastability of spinel-type solid solutions in the SiO_2 - Al_2O_3 system. *Chem. Mater.*, 1997, **9**, 3096–3100.
24. Douy, A., *Stabilisation of Transition Aluminas by Alkaline Earth Ions*, in *Euroceramics V, vol 1*, ed. D. Bortzmeier, M. Boussuge, Th. Chartier, G. Fantozzi, G. Lozes and A. Rousset. Trans Tech Publications, Zurich, Switzerland, 1997, pp. 101–104.
25. Gerardin, C., Sundaresan, S., Benziger, J. and Navrotsky, A., Structural investigation and energetics of mullite formation from sol-gel precursors. *Chem. Mater.*, 1994, **6**, 160–170.
26. Tkalcec, E., Nass, R., Schmauch, J., Schmidt, H., Kurajica, S., Bezjak, A. *et al.*, Crystallization kinetics of mullite from single-phase gel determined by isothermal differential scanning calorimetry. *J. Non-Cryst. Solids*, 1998, **223**, 57–72.
27. Okada, K., Kaneda, J-I., Kameshima, Y., Yasumori, A. and Takei, T., Crystallization kinetics of mullite from polymeric Al_2O_3 - SiO_2 xerogels. *Mater. Lett.*, 2003, **4304**, 1–5.
28. Tkalcec, E., Ivankovic, H., Nass, R. and Schmidt, H., Crystallization kinetics of mullite formation in diphasic gels containing different alumina components. *J. Eur. Ceram. Soc.*, 2003, **23**, 1465–1475.
29. Huling, J. C. and Messing, G. L., Epitactic nucleation of spinel in aluminosilicate gels and its effect on mullite crystallization. *J. Am. Ceram. Soc.*, 1991, **74**, 2374–2381.
30. Sacks, M. D., Wang, K., Scheiffele, G. W. and Bozkurt, N., Activation energy for mullitization of α -alumina/silica microcomposite particles. *J. Am. Ceram. Soc.*, 1996, **79**, 571–573.
31. Aksay, I. and Pask, J. A., Stable and metastable equilibria in the system SiO_2 - Al_2O_3 . *J. Am. Ceram. Soc.*, 1975, **58**, 507–512.
32. Horiuchi, T., Chen, L., Osaki, T., Sugiyama, T., Suzuki, K. and Mori, T., A novel alumina catalyst support with high thermal stability derived from silica-modified alumina gel. *Catal. Lett.*, 1999, **58**, 89–92.